Cellulose (2018) 25:1809–1819
https://doi.org/10.1007/s10570-018-1651-4

ORIGINAL PAPER

Carbon/ZnO nanorods composites templated by TEMPO-oxidized cellulose and photocatalytic activity for dye degradation

He Xiao · Weibo Zhang · Yicui Wei · Lihui Chen

Received: 20 October 2017 / Accepted: 4 January 2018 / Published online: 10 January 2018

Abstract Zinc oxide (ZnO) is among the most interesting metal oxide with remarkable performance in electronics, semiconducting materials and photocatalysis, specially as nanomaterials. In this work, carbon/ZnO nanocomposites were designed using a low temperature precipitation process and TEMPO-oxidized (2,2,6,6-Tetramethyl-1-piperidinyloxy as TEMPO) cellulose as a reactive template. The resulting nanomaterials were characterized by XRD, SEM, TEM, BET, EDX and UV–vis spectroscopy analysis. It was found that the formation of carbon/ZnO nanocomposites with various morphologies not only involved the structure of TEMPO-oxidized cellulose but also depended on the content of the carboxyl groups of TEMPO-oxidized cellulose. In this approach, TEMPO-oxidized cellulose is not only a template provider, but is a C-provider leading to a compound into the ZnO nanocrystals which were decreased the band gaps of samples. ZnO-T12 exhibited a significant photodegradation on methyl orange with 96.11% within 120 min and good reusability.

Keywords ZnO · TEMPO-oxidized cellulose · Photocatalyst · Template

Introduction

Over the past few decades, environmental and energy problems have attracted worldwide attention, especially, wastewater has become a threat of ecological crisis (Mehrjouei et al. 2015; Xiao et al. 2015; Teh et al. 2017). Traditional treatment of wastewater usually involves adsorption and coagulation (Nair et al. 2014; Teh et al. 2016) however, these methods only transfer or condense these contaminants but which are decomposed and required additional treatment to avoid secondary pollution (Liu et al. 2016b). Photocatalysis, a clean and efficient technology, has been widely used for wastewater treatment (Yao et al. 2016; Wang et al. 2016), gas degradation (Sano et al. 2013; Zhang et al. 2010) and is also potentially a route to the production of chemicals and fuels. It requires photocatalyst that must be cheap, non-toxic, easy to handle and above all efficient (Lv et al. 2016; Wang et al. 2017).

Zinc oxide (ZnO) is among the most appealing ones, being an n-type semiconductor with a wide band gap and is commonly used as a photocatalyst for contaminants degradation because of its unique electronic structure (Yu et al. 2016; Jo and Selvam 2015). As a photocatalyst, specific surface area plays an

Electronic supplementary material The online version of this article (https://doi.org/10.1007/s10570-018-1651-4) contains supplementary material, which is available to authorized users.

H. Xiao (✉) · W. Zhang · Y. Wei · L. Chen
College of Materials Engineering, Fujian Agriculture and Forestry University, Fuzhou 350002, China
e-mail: Xiaohe_river@163.com

important role in the photocatalytic performance since by determining the number of active sites and the distance between the sites of photon absorption and electron/hole redox in order to enhance photocatalytic efficiency (Saikia et al. 2017; Ge et al. 2017). The facets exposed are also of great importance since not all of them present the same active species and their redox-potential. Thus, much attention has been paid to the synthesis of ZnO with morphology-controlled methods (Boury and Plumejeau 2015; Xia et al. 2016), such as nanotubes (Samadipakchin et al. 2017), nanorods (Liu 2016), nanowires (Chang 2014), nanospheres (Song et al. 2016) etc. Until now, different methods, such as hydrothermal process, sol–gel (Khodadadi et al. 2016), magnetron sputtering (Perez-Gonzalez et al. 2017) and chemical vapor deposition (Wang et al. 2012) have been used to prepare ZnO photocatalysts. Templated-directed mineralization is a promising nanofabrication technique because both physical and chemical cues from the template could control over the size and structure of the resulting materials (Ceylan et al. 2013). Recently, researchers have prepared some novel ZnO doping with metal Fe^{2+} (Ambika et al. 2016), AgNPs (Basuny et al. 2015) in order to enhance the photocatalytic activity. Additionally, biomass template not only fabricates ZnO advanced materials, but provides carbon sources doping ZnO (Zhao et al. 2017; Wang et al. 2014).

Cellulose is one of the most utilized and cheapest polysaccharides which is used as both chelating and stabilizing agents because of its abundant hydroxyl groups which support affinities and active sites to the precursors and growth of inorganic nanoparticles (Liu et al. 2011; Lidor-Shalev et al. 2017). Additionally, cellulose is a potentially reducing agent in the formation of metal nanoparticles such as Ag, Au and Pt (Boury and Plumejeau 2015). In the past, it has been already used as a template for the preparation of ZnO and the formation of ZnO/cellulose was reported (Lefatshe et al. 2017; Yuan et al. 2017). Cellulose is also known as being selectively oxidized by 2,2,6,6-Tetramethyl-1-piperidinyloxy (TEMPO) agent that reacts with the primary hydroxyl groups (C-6) and oxidizes it into carboxyl groups (Saito et al. 2007). Two additional points must be considered: first, in solution, it is easier to form carboxylate than hydroxylate and secondly, it is known that carboxylate can better coordinate metal cations than do hydroxyl function. Therefore, TEMPO-oxidized cellulose should have stronger adsorption capacity toward coordination of Zn^{2+}. We thought attractive to see if such enhanced reactivity can speed up, limit or orient the growth of growth of nanocrystals (Foresti et al. 2017; Liu et al. 2016a) in order to finally obtain ZnO nanomaterials with highly active crystal phase in optimal conditions. We check the effect of the carboxylate content by controlling the TEMPO oxidation. Interestingly, we found that this carboxylate content has also an impact on the C-content of the ZnO after calcination at 400 °C. It thus appears that we came across a simple process to access to carbon/ZnO nanocomposites. The effect of such treatment of the corresponding material was checked by looking to their photocatalytic activity estimated using methyl orange solution as target degradation molecule, the latter being commonly used in the photodegradation tests and allowing comparison (Khan et al. 2015; Danwittayakul et al. 2013).

In this paper, carbon/ZnO nanocomposites were successfully synthesized by using cellulose as a template but previously oxidized by TEMPO in agreement with well known method (Isogai et al. 2011). The chemical composition, crystallinity and morphology of carbon/ZnO nanocomposites were investigated by XRD-ray, BET, EDX, SEM and TEM etc. Effects of type of TEMPO-oxidized cellulose on photocatalytic degradation of methyl orange were also investigated.

Materials and methods

Materials

Zinc nitrate hexahydrate, urea, sodium hypochlorite, sodium bromide and sodium hydroxide, hydrochloric acid, absolute ethanol were of analytical grade and utilized without purification. TEMPO agent (98%) and methyl orange (96%) were obtained from Aladdin Industrial Corporation. Bamboo dissolving pulp (α-cellulose $\geq$ 95%) was obtained from Fujian Qingshan Paper Industry Co., Ltd. The bamboo cellulose fiber, a common fast-growing non-wood in southern China, was used to prepare TEMPO-oxidized cellulose without pretreatment before experiment.

Preparation of TEMPO-oxidized cellulose

Bamboo pulp (5.00 g) was dispersed in deionized water (500 mL) at room temperature (20 °C) using mechanical stirring (500 r/min) for 2 h. Then 2,2,6,6-tetramethylpiperidine-1-oxyl (TEMPO solution in water, 0.1 mmol/g) and sodium bromide (NaBr in water, 1.0 mmol/g) were added into the suspension. Then sodium hypochlorite (NaClO in water, x mmol/g) was added drop by drop and pH was maintained at about 10 using sodium hydroxide solution (NaOH in water, 0.1 mmol/L). The obtained suspension was stirred (300 r/min) for 6 h at 20 °C and terminated by neutralization of hydrochloric acid in order to obtain pH 7. The wet TEMPO-oxidized cellulose fiber was then centrifuged at 10,000 r/min for 20 min and collected. Finally, the sample was freezing-dried at − 50 °C for 24 h. The final products were named for Blank, T3, T6 and T12, respectively according to the amount of NaClO (0, 3, 6, 12 mmol/g). Carboxyl contents in the TEMPO-oxidized celluloses were determined by the electric conductivity titration method (Saito and Isogai 2004).

Preparation of carbon/ZnO nanocomposites with TEMPO-oxidized cellulose

TEMPO-oxidized cellulose (1.89 g, as 1 wt.% water suspension) was dispersed in a 250 mL round bottomed flask with water (150 mL) and Zinc nitrate ($Zn(NO_3)_2{\cdot}6H_2O$, 2.97 g, 10 mmol) was added and magnetically stirred (400 r/min) for 2 h at 30 °C. Then urea (CH_4ON_2, 0.36 g, 6 mmol) was dissolved in the mixture. The latter was warmed in an oil bath at 90 °C for 4 h. After being cooled down, the suspension was centrifugated (8000 r/min) in order to obtain crude product, and washed with deionized water and absolute ethanol (two times, successively) and then vacuum dried at 50 °C for 24 h. Finally, the dried products were calcined at 400 °C in air atmosphere for 2 h, leading respectively to samples ZnO-FT, ZnO-T3, ZnO-T6 and ZnO-T12. The synthesis routes of carbon/ZnO nanocomposites were shown in Fig. 1.

Characterizations

Optical morphologies of TEMPO-oxidized cellulose were determined by fiber analyzer (Techpap,MorFi Compact,France). X-ray diffraction (XRD) analysis was carried out by X-ray diffractometer (Rigaku, Ultima IV, Japan) using Cu Kα radiation, tube voltage 40 kV and tube current 45 mA. A field emission scanning electron microscope (Hitachi, SU8010, Japan) was used to observe the surface morphology and microstructure of carbon/ZnO samples. The detailed microstructures of all the samples were investigated by using a (JEOL, JEM-2100, Japan) transmission electron microscopy (TEM) with a field emission gun operating at 200 kV. The specific surface area and pore characteristics of carbon/ZnO samples were measured by N_2 adsorption–desorption specific surface area analyzer (Micromeritics, ASAP 2020, USA). The chemical compositions of carbon/ZnO samples were studied by energy dispersive spectroscopy (HORIBA, XMX 1011, Japan). Diffuse reflectance UV–Vis (DR UV–Vis) spectra were recorded on Cary 500, Varian Corporation.

Evaluation of photocatalytic activity

The photocatalytic source was launched out by ultraviolet lamp with power about 36 W. The distance between the light source and the reaction tube was 10 cm. Many dyes are visible in water at concentrations as low as 1 mg/L, which is enough to present an aesthetic problem (Low et al. 2012; Subramonian and Wu 2014). In this study, a mixture containing of carbon/ZnO (25 mg, 0.309 mmol) was added to a solution of methyl orange (100 mL of MO in aqueous solution, 5 mg/L), magnetically stirred (300 r/min) at 30 °C for 30 min in the dark and irradiated range from 0 to 120 min without feeding oxygen. Then, irradiation was started and samples of 4 mL were withdrawn and filtered through a 0.22 μm PES membrane (Jin Teng Experimental Equipment Co., Ltd., 13 × 0.22 μm, Tianjin, China) at 15, 30, 60, 90 and 120 min, respectively. During the illumination, no additional oxygenation was introduced. The absorbance of the filtrate was measured by UV–Vis spectrophotometer (Shimadzu, UVmini-1240, Japan).

Fig. 1 The schematic illustration of the fabrication of carbon/ZnO nanocomposites templated by TEMPO-oxidized cellulose

Results and discussion

Characteristics of different TEMPO-oxidized cellulose

Treatment of cellulose by TEMPO/NaClO was performed with different amount of NaClO (Fig. 2) with the aim to show its effect on the morphologies of the cellulose and carboxylic content. As expected, increasing of the amount of NaClO, result in an increase of the carboxyl groups content from 0.105 to 1.478 mmol/g as shown in Table 1. These new carboxyl groups are favorable for the reaction with zinc precursor as reported (Qian et al. 2012).

However, the oxidation process has another effect that is to shorten the fibers, a process that is ascribed to hydrolysis/oxidation of some less thick part of the fiber. Indeed, increasing the NaClO lead to an average decrease of the average fibers' length from 1.559 to 0.361 mm with no important change of the diameter. Meanwhile, the ratio of length to width dropped from 66 to 15.

Characteristics of carbon/ZnO nanocrystals templated by TEMPO-oxidized cellulose

The crystalline phases of carbon/ZnO samples templated by TEMPO-oxidized cellulose are characterized by XRD measurements. For comparison, pure ZnO sample (ZnO-FT), which was without the use of TEMPO-oxidized cellulose is also tested. As shown in Fig. 3, after calcination, both ZnO-FT and ZnO-T exhibit the uniform wurtzite structure with characteristic 2θ values at (31.96°, 34.60°, 36.46°, 47.74°, 56.78°, 63.06°, 66.52°, 68.16°, 69.26°). The diffraction peaks originated from TEMPO-oxidized cellulose template are hardly detected in carbon/ZnO samples. Moreover, there is no remarkable shift of all diffraction peaks. To further investigate the crystallization characteristics of carbon/ZnO samples templated by TEMPO-oxidized cellulose, crystalline size from three main crystal planes were shown in (supporting information Table 1). Crystalline size of carbon/ZnO became smaller after template synthesis process due to oriental induction of TEMPO-oxidized cellulose rich in carboxyl and hydroxyl groups (Goncalves et al. 2009; Costa et al. 2013). Thus, these carbon/ZnO samples had potential advantage of the photodegradation of wastewater (Kumaresan et al. 2017).

Figure 4 shows that the SEM images of the carbon/ZnO samples after calcination. It can be observed that they all present a similar morphology resulting from aggregated lamella. However, the carbon/ZnO sample prepared with the highest carboxylate-content present a remarkable difference, the lamella being less packed and aggregated. ZnO samples are composed of multidimensional structures. After calcinations process, the ZnO prepared by template method gradually

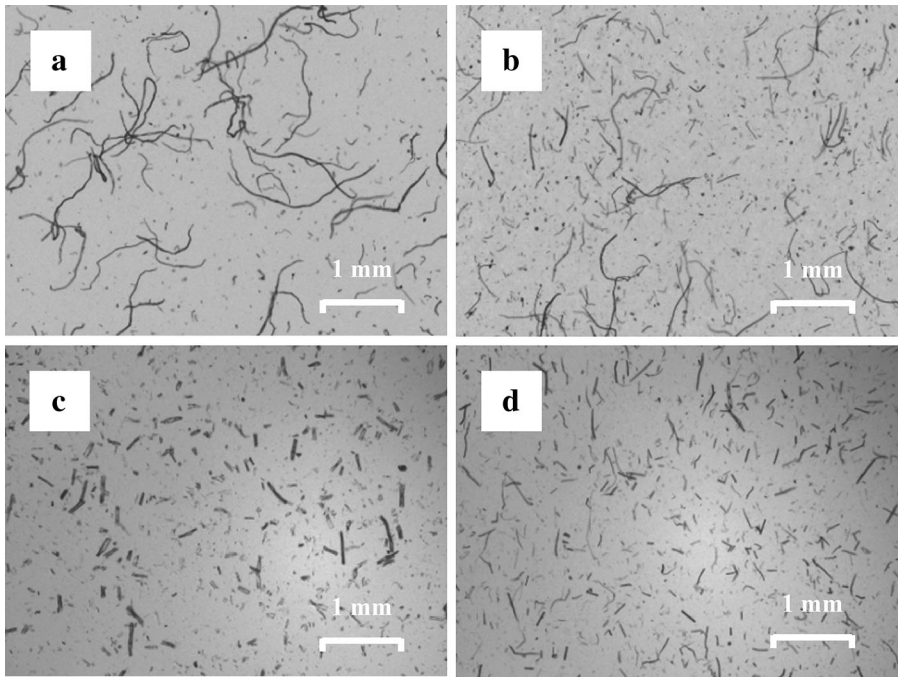

Fig. 2 Photographs of TEMPO-oxidized cellulose with different amounts of NaClO (**a** 0 mmol/g, **b** 3 mmol/g, **c** 6 mmol/g, **d** 12 mmol/g)

Table 1 Characteristics of different TEMPO-oxidized cellulose

Samples	NaClO amount (mmol/g)	Weight-average length (mm)	Width (μm)	Length–width ratio	Carboxyl content (mmol/g)
Blank	0	1.559	23.6	66.06	0.105
T3	3	1.057	17.8	59.38	0.248
T6	6	0.447	32.7	13.67	0.828
T12	12	0.361	23.0	15.70	1.478

changed from nanosheets to nanorods with the increase of carboxyl of TEMPO-oxidized cellulose. In our work, uniformly distributed carboxyl groups of TEMPO-oxidized cellulose can coordinate with Zn^{2+} to form stable and dispersive ZnO nanograins, and the polymer network prevent ZnO nanoparticles from agglomeration efficiently at the same time. So, the ZnO nanorods had been formed by TEMPO-oxidized cellulose as templates. However, the original cellulose has not to prevent the agglomeration of ZnO nanoparticles because of weak bonding between hydroxyl groups and Zn^{2+}. Moreover, ZnO nanoparticles have not grown in orient direction along the original cellulose because of its larger size (Li et al. 2009; Zhao et al. 2017). Herein, ZnO nanosheets had been formed by original cellulose.

The carbon/ZnO samples are further confirmed by Brunauer–Emmett–Teller (BET) measurements and the N_2 adsorption–desorption isotherms are shown in Fig. 5. The samples displayed a typical isotherm curve with an obvious hysteresis loop at high relative pressure ($P/P_0 = 0.985$), indicating the presence of mesoporous materials that probably results from intergranular void between lamella particles. The pore size distribution is determined by Barrett–Joyner–Halenda (BJH) analysis of the desorption branch of the isotherm from Fig. 4. It can be seen from Table 2 that the BET surface area does not increases with the

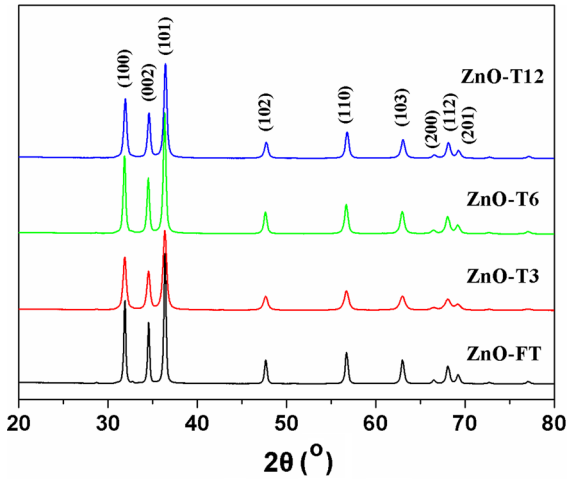

Fig. 3 XRD patterns of carbon/ZnO nanocrystals templated by different TEMPO-oxidized cellulose

content of carboxyl groups, except for the sample prepared with the highest carboxylate content; this fact being in agreement with the SEM observations. The large surface area and porosity will contribute to the photocatalytic activity (Chen et al. 2013a; Subramonian et al. 2017).

From Energy-dispersive X-ray (EDX) characterization, all samples of carbon/ZnO templated by TEMPO-oxidized cellulose were investigated. It can be seen from Fig. 6 that ZnO samples were composed of zinc, oxygen and carbon. The presence of the latter because the calcination temperature was only 400 °C and with the increase of carboxyl content, the more residual carbon element was embedded into the ZnO samples. Zinc ions, the precursor of ZnO samples, could be adsorbed preferentially to the TEMPO-oxidized cellulose with more carboxyl groups. Thus, TEMPO-oxidized cellulose can combine the ZnO samples more closely. After calcinations, residual carbon from template was compounded into the ZnO samples, playing an important role to improve the photocatalytic activity.

Photocatalytic activity of carbon/ZnO nanocrystals for methyl orange degradation

The UV–vis DR spectra of the as-prepared mesoporous carbon/ZnO samples are shown in Fig. 7a, b. By increasing the content of carboxyl groups of TEMPO-oxidized cellulose, the UV–vis DR spectra of carbon/ZnO by template are slightly shifted to visible light as compared with ZnO free of template (ZnO-FT). The absorbance edge of the ZnO by template is shifted from 417 nm to 432 nm (shown in supporting information Table 2) when the content of carboxyl groups is increased from 0.105 to 1.478 mmol/g, due to the fact that the carbon compounded into the ZnO crystals can slightly increase the light absorption ability. The band gap energy of the ZnO samples were calculated from the UV–vis DR spectra as following the formula: $E_g = 1240/\lambda_g$, where E_g (eV) is the band gap energy, λ_g (nm) is absorbance edge. From Fig. 6b, along with the increase of the content of carboxyl groups from 0.105 to 1.478 mmol/g, the band gap energy of carbon/ZnO samples were decreased from 2.97 to 2.87 eV.

Photodegradation experiments of MO were studied under UV to investigate photocatalytic activity of ZnO templated by TEMPO-oxidized cellulose. Figure 7c displays the testing results for ZnO templated by TEMPO-oxidized cellulose with different carboxylate contents. It was observed that MO removal rate significantly increased by the carboxylate amount of cellulose template. Activity are similar whatever are the carboxylate content used for the preparation of the sample, as long as it reach the highest carboxylate contents of 1.478 mmol/g that clearly leads to a much better photocatalytic activity increased by a factor $\approx$ 2. After dark reaction, methyl orange only decreased by 1–2%. While the methyl orange photodegradation by ZnO-FT, ZnO-T3, ZnO-T6 and ZnO-T12 decreased by 65.92, 71.19, 72.76 and 96.11%, respectively. This is because ZnO-T12 with high surface area and narrow band was templated from TEMPO-oxidized cellulose with high content of carboxyl groups, making it easier to contact with pollutants and inspire more electron hole pairs to increase the photodegradation activity. The photocatalytic performance for degradation of methyl orange in the present work is superior to the previous reported (Yan et al. 2015; Chen et al. 2013b). Figure 7d shows the reusability of ZnO samples for photocatalytic degradation of methyl orange. It can be seen that ZnO-FT and ZnO-T12 samples have good photocatalytic stability. Methyl orange had been removed 38.68 and 79.78% initially by ZnO-FT and ZnO-T12, respectively. After 5 times for photodegradation, methyl orange can still hold 30.50 and 70.53% removal by ZnO-FT and ZnO-T12, respectively.

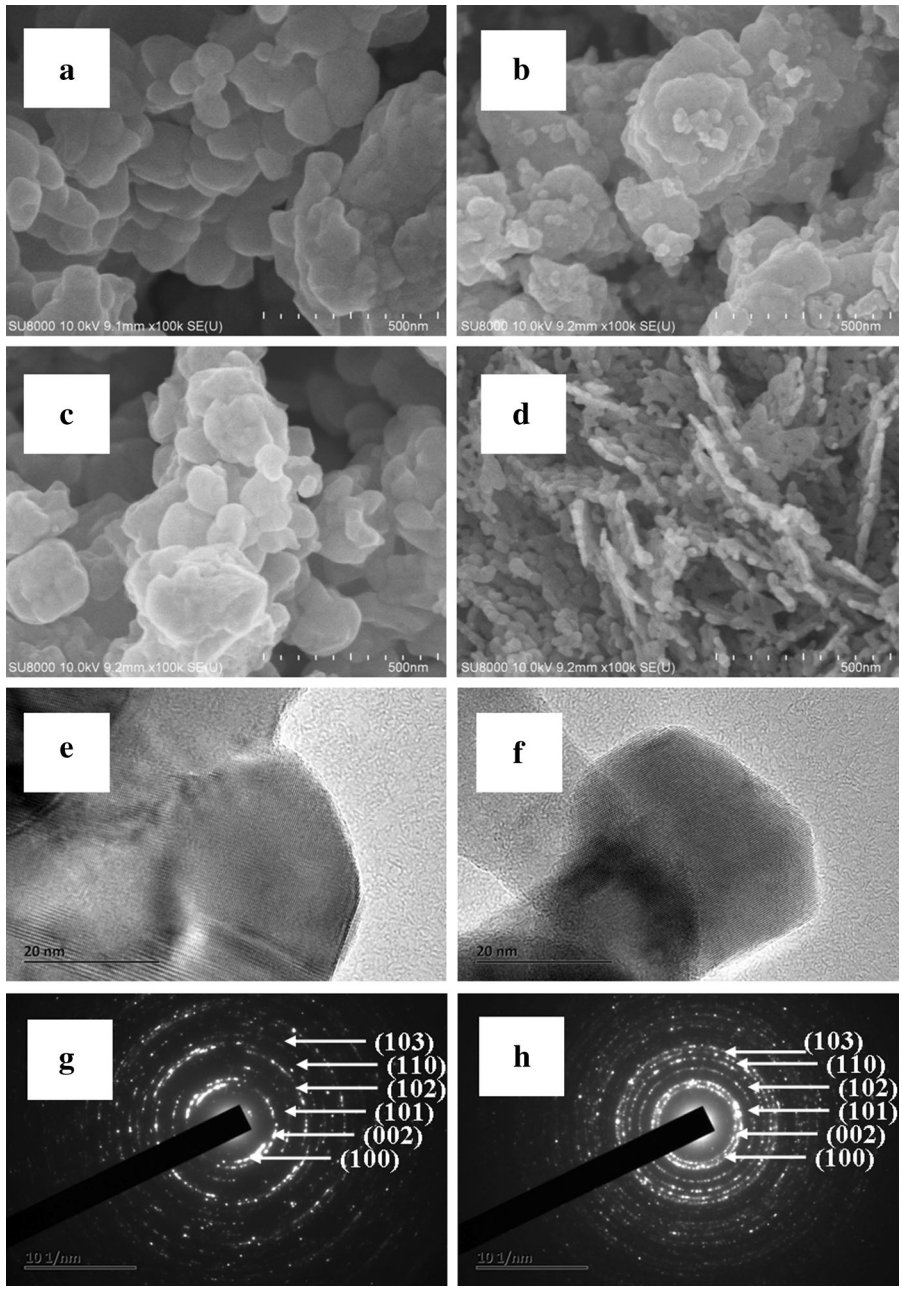

Fig. 4 SEM images of ZnO-FT (**a**), ZnO-T3 (**b**), ZnO-T6 (**c**) and ZnO-T12 (**d**), TEM images of ZnO-FT (**e**) and ZnO-T12 (**f**), SAED images of ZnO-FT (**g**) and ZnO-T12 (**h**)

Figure 7e, f show full wavelength curves for photocatalytic degradation of methyl orange at different times of ZnO-T12 and ZnO-FT, respectively. It can be seen that the degradation rate of ZnO-T12 for methyl orange was significantly faster than ZnO-FT. With the extension of time, on the one hand, the maximum absorption peak of 463 nm became smaller indicating that the methyl orange concentration decreased; on the other hand, the absorption peak at 463 nm shifted to shorter wavelengths, implying that methyl orange degradation into other molecules (Kaur and Singhal 2014).

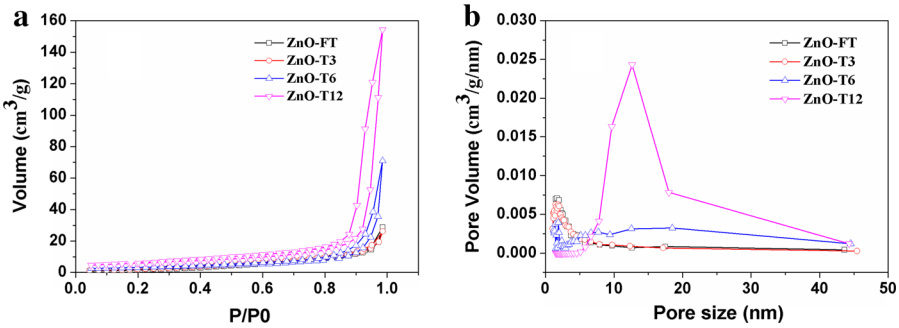

Fig. 5 N_2 adsorption–desorption isotherms of carbon/ZnO samples (**a**) and pore size distribution derived from desorption isotherm (**b**)

Table 2 Characteristics of the carbon/ZnO templated by different TEMPO-oxidized cellulose

Samples	Surface area (m^2/g)	Pore volume (cm^3/g)	Pore size (nm)
ZnO-FT	9.72	0.04	9.20
ZnO-T3	11.17	0.11	19.69
ZnO-T6	10.79	0.04	7.54
ZnO-T12	20.60	0.24	23.23

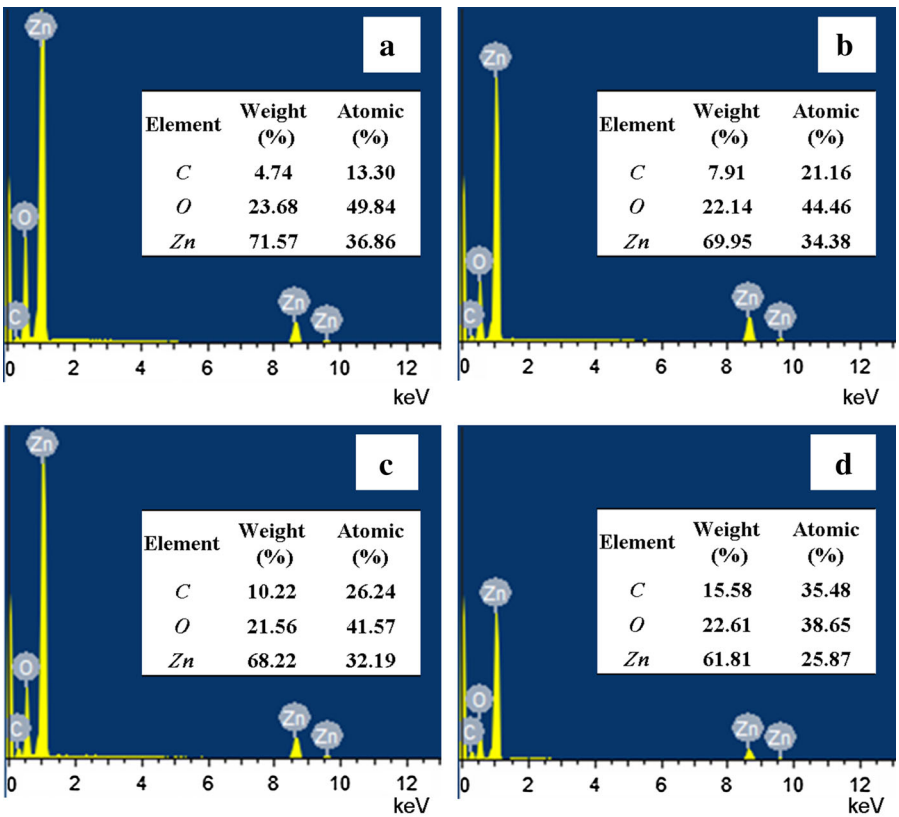

Fig. 6 EDX spectra of ZnO-FT (**a**), ZnO-T3 (**b**), ZnO-T6 (**c**) and ZnO-T12 (**d**)

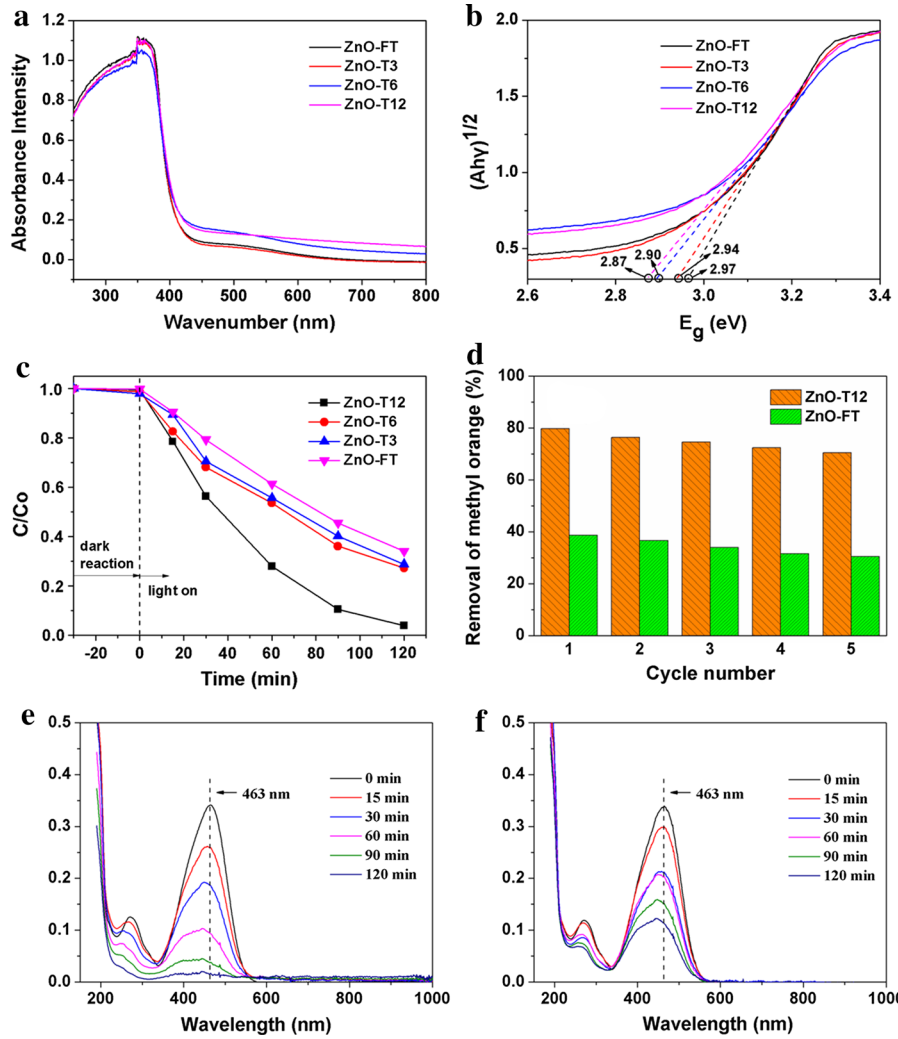

Fig. 7 UV-Vis DR spectra for carbon/ZnO samples (**a**), UV–vis relationship between band gap energy and $[Ah\gamma]^{1/2}$ of all the samples (**b**), photocatalytic activity of carbon/ZnO samples (**c**), reusability of ZnO-FT and ZnO-T12 on photocatalytic activity (**d**), photocatalytic activity of ZnO-T12 (**e**) and ZnO-FT (**f**) with different reaction time

Conclusions

The novel carbon/ZnO photocatalyst had been successfully prepared via precipitation approach using TEMPO-oxidized cellulose as soft template. On the morphological structure, the ZnO samples were significantly affected by the addition of TEMPO-oxidized cellulose. The crystalline size of ZnO-T was smaller than that of ZnO-FT. And the surface area and pore volume of ZnO-T was increased at the same time. On the chemical characteristics, more carbon from TEMPO-oxidized cellulose was compounded into the ZnO crystals so that the band gap energy of ZnO had been narrowed resulting enhanced photocatalytic activity. Therefore, T12 was considered as the best bio-template to exhibit appropriate microstructure and chemical properties. ZnO-T12 displayed the highest photocatalytic activity in the degradation of methyl orange under UV irradiation with 96.11% degradation of methyl orange and good stability for five cycles.

Acknowledgments This work was supported by Natural Science Foundation of China (31700519), Science Fund of Fujian Provincial University (JK2017013), Fujian Science and Technology of Education Department Fund (JAT160151), Fujian Innovation and Entrepreneurship Training Program (201710389035).

References

Ambika S, Nambi IM, Senthilnathan J (2016) Low temperature synthesis of highly stable and reusable CMC-Fe2 + (-

nZVI) catalyst for the elimination of organic pollutants. Chem Eng J 289:544–553

Basuny M, Ali IO, Abd El-Gawad A et al (2015) A fast green synthesis of Ag nanoparticles in carboxymethyl cellulose (CMC) through UV irradiation technique for antibacterial applications. J Sol-Gel Sci Technol 75(3):530–540

Boury B, Plumejeau S (2015) Metal oxides and polysaccharides: an efficient hybrid association for materials chemistry. Green Chem 17(1):72–88

Ceylan H, Ozgit-Akgun C, Erkal TS et al (2013) Size-controlled conformal nanofabrication of biotemplated three-dimensional TiO_2 and ZnO nanonetworks. Sci Rep 3:2306

Chang Y (2014) Low temperature growth of ZnO nanowire arrays with enhanced high performance photocatalytic activity and reusability. Catal Commun 56:45–49

Chen S, Zhou B, Hu W et al (2013a) Polyol mediated synthesis of ZnO nanoparticles templated by bacterial cellulose. Carbohyd Polym 92(2):1953–1959

Chen YL, Kuo L, Tseng ML et al (2013b) b) ZnO nanorod optical disk photocatalytic reactor for photodegradation of methyl orange. Opt Express 21(6):7240–7249

Costa SV, Goncalves AS, Zaguete MA et al (2013) ZnO nanostructures directly grown on paper and bacterial cellulose substrates without any surface modification layer. Chem Commun 49(73):8096–8098

Danwittayakul S, Jaisai M, Koottatep T et al (2013) Enhancement of photocatalytic degradation of methyl orange by supported zinc oxide nanorods/zinc stannate (ZnO/ZTO) on porous substrates. Ind Eng Chem Res 52(38):13629–13636

Foresti ML, Vazquez A, Boury B (2017) Applications of bacterial cellulose as precursor of carbon and composites with metal oxide, metal sulfide and metal nanoparticles: a review of recent advances. Carbohyd Polym 157:447–467

Ge M, Li Q, Cao C, et al (2017) One-dimensional TiO_2 nanotube photocatalysts for solar water splitting. Adv Sci 4(1):1600 152–1600182

Goncalves G, Marques PAAP, Neto CP et al (2009) Growth, structural, and optical characterization of ZnO-coated cellulosic fibers. Cryst Growth Des 9(1):386–390

Isogai A, Saito T, Fukuzumi H (2011) TEMPO-oxidized cellulose nanofibers. Nanoscale 3(1):71–85

Jo W, Selvam NCS (2015) Enhanced visible light-driven photocatalytic performance of ZnO-g-C3N4 coupled with graphene oxide as a novel ternary nanocomposite. J Hazard Mater 299:462–470

Kaur J, Singhal S (2014) Facile synthesis of ZnO and transition metal doped ZnO nanoparticles for the photocatalytic degradation of Methyl Orange. Ceram Int 40(5):7417–7424

Khan R, Hassan MS, Uthirakumar P et al (2015) Facile synthesis of ZnO nanoglobules and its photocatalytic activity in the degradation of methyl orange dye under UV irradiation. Mater Lett 152:163–165

Khodadadi B, Bordbar M, Yeganeh-Faal A (2016) Optical, structural, and photocatalytic properties of Cd-doped ZnO powders prepared via sol–gel method. J Sol-Gel Sci Technol 77(3):521–527

Kumaresan N, Ramamurthi K, Babu RR et al (2017) Hydrothermally grown ZnO nanoparticles for effective photocatalytic activity. Appl Surf Sci 418:138–146

Lefatshe K, Muiva CM, Kebaabetswe LP (2017) Extraction of nanocellulose and in situ casting of ZnO/cellulose nanocomposite with enhanced photocatalytic and antibacterial activity. Carbohyd Polym 164:301–308

Li J, Li L, Xu J et al (2009) Controlled growth of ZnO nanorods by polymer template and their photoluminescence properties. Sci China Ser E Technol Sci 52(4):888–892

Lidor-Shalev O, Pliatsikas N, Carmiel Y et al (2017) Chiral metal-oxide nanofilms by cellulose template using atomic layer deposition process. ACS Nano 11(5):4753–4759

Liu L (2016) Controllable ZnO nanorod arrays@carbon fibers composites: towards advanced CO2 photocatalytic reduction catalysts. Ceram Int 42(10):12516–12520

Liu S, Ke D, Zeng J et al (2011) Construction of inorganic nanoparticles by micro-nano-porous structure of cellulose matrix. Cellulose 18(4):945–956

Liu P, Oksman K, Mathew AP (2016a) Surface adsorption and self-assembly of Cu(II) ions on TEMPO-oxidized cellulose nanofibers in aqueous media. J Colloid Interface Sci 464: 175–182

Liu Y, Duan J, Li W et al (2016b) Effects of organic matter removal from a wastewater secondary effluent by aluminum sulfate coagulation on haloacetic acids formation. Environ Eng Sci 33(7):484–493

Low FCF, Wu TY, Teh CY et al (2012) Investigation into photocatalytic decolorisation of CI Reactive Black 5 using titanium dioxide nanopowder. Color Technol 128(1):44–50

Lv Y, Cao X, Jiang H et al (2016) Rapid photocatalytic debromination on TiO_2 with in situ formed copper co-catalyst: enhanced adsorption and visible light activity. Appl Catal B-Environ 194:150–156

Mehrjouei M, Mueller S, Moeller D (2015) A review on photocatalytic ozonation used for the treatment of water and wastewater. Chem Eng J 263:209–219

Nair V, Panigrahy A, Vinu R (2014) Development of novel chitosan-lignin composites for adsorption of dyes and metal ions from wastewater. Chem Eng J 254:491–502

Perez-Gonzalez M, Tomas SA, Santoyo-Salazar J et al (2017) Enhanced photocatalytic activity of TiO2-ZnO thin films deposited by dc reactive magnetron sputtering. Ceram Int 43(12):8831–8838

Qian Y, Qin Z, Ngoc-Minh V et al (2012) Comparison of nanocrystals from TEMPO oxidation of bamboo, softwood, and cotton linter fibers with ultrasonic-assisted process. BioResources 7(4):4952–4964

Saikia H, Borah BJ, Yamada Y et al (2017) Enhanced catalytic activity of CuPd alloy nanoparticles towards reduction of nitroaromatics and hexavalent chromium. J Colloid Interface Sci 486:46–57

Saito T, Isogai A (2004) TEMPO-mediated oxidation of native cellulose. The effect of oxidation conditions on chemical and crystal structures of the water-insoluble fractions. Biomacromol 5(5):1983–1989

Saito T, Kimura S, Nishiyama Y et al (2007) Cellulose nanofibers prepared by TEMPO-mediated oxidation of native cellulose. Biomacromol 8(8):2485–2491

Samadipakchin P, Mortaheb HR, Zolfaghari A (2017) ZnO nanotubes: preparation and photocatalytic performance evaluation. J Photochem Photobiol A Chem 337:91–99

Sano T, Tsutsui S, Koike K et al (2013) Activation of graphitic carbon nitride (g-C3N4) by alkaline hydrothermal treatment for photocatalytic NO oxidation in gas phase. J Mater Chem A 1(21):6489–6496

Song Y, Shao P, Tian J et al (2016) One-step hydrothermal synthesis of ZnO hollow nanospheres uniformly grown on graphene for enhanced photocatalytic performance. Ceram Int 42(1B):2074–2078

Subramonian W, Wu TY (2014) Effect of enhancers and inhibitors on photocatalytic sunlight treatment of methylene blue. Water Air Soil Pollut 225:19224

Subramonian W, Wu TY, Chai S (2017) Photocatalytic degradation of industrial pulp and paper mill effluent using synthesized magnetic Fe2O3-TiO2: treatment efficiency and characterizations of reused photocatalyst. J Environ Manage 187:298–310

Teh CY, Budiman PM, Shak KPY et al (2016) Recent advancement of coagulation-flocculation and its application in wastewater treatment. Ind Eng Chem Res 55(16):4363–4389

Teh CY, Wu TY, Juan JC (2017) An application of ultrasound technology in synthesis of titania-based photocatalyst for degrading pollutant. Chem Eng J 317:586–612

Wang SL, Zhu HW, Tang WH, Li PG (2012) Propeller-Shaped ZnO nanostructures obtained by chemical vapor deposition: photoluminescence and photocatalytic properties. J Nanomater. https://doi.org/10.1155/2012/594290

Wang X, Zhang Y, Hao C et al (2014) Solid-phase synthesis of mesoporous zno using lignin-amine template and its photocatalytic properties. Ind Eng Chem Res 53(16):6585–6592

Wang H, Yuan X, Wu Y et al (2016) In situ synthesis of In2S3@MIL-125(Ti) core-shell microparticle for the removal of tetracycline from wastewater by integrated adsorption and visible-light-driven photocatalysis. Appl Catal B-Environ 186:19–29

Wang J, Chen Y, Liu G et al (2017) Synthesis, characterization and photocatalytic activity of inexpensive and non-toxic Fe2O3-Fe3O4 nano-composites supported by montmorillonite and modified by graphene. Compos B-Eng 114:211–222

Xia Y, Wang J, Chen R et al (2016) A review on the fabrication of hierarchical ZnO nanostructures for photocatalysis application. Crystals 6:14811

Xiao J, Xie Y, Cao H (2015) Organic pollutants removal in wastewater by heterogeneous photocatalytic ozonation. Chemosphere 121:1–17

Yan C, Lina Z, Lichao N et al (2015) Superior photocatalytic activity of porous wurtzite ZnO nanosheets with exposed (0 0 1) facets and a charge separation model between polar (0 0 1) and (0 0 1) surfaces. Chem Eng J 264:557–564

Yao Y, Chen H, Lian C et al (2016) Fe Co, Ni nanocrystals encapsulated in nitrogen-doped carbon nanotubes as Fenton-like catalysts for organic pollutant removal. J Hazard Mater 314:129–139

Yu W, Zhang J, Peng T (2016) New insight into the enhanced photocatalytic activity of N-, C- and S-doped ZnO photocatalysts. Appl Catal B-Environ 181:220–227

Yuan Y, Fu A, Wang Y et al (2017) Spray drying assisted assembly of ZnO nanocrystals using cellulose as sacrificial template and studies on their photoluminescent and photocatalytic properties. Colloids Surf A Physicochem Eng Asp 522:173–182

Zhang Y, Tang Z, Fu X et al (2010) TiO2-graphene nanocomposites for gas-phase photocatalytic degradation of volatile aromatic pollutant: is TiO2-graphene truly different from other TiO2-carbon composite materials. ACS Nano 4(12):7303–7314

Zhao S, Zuo H, Guo Y et al (2017) Carbon-doped ZnO aided by carboxymethyl cellulose: fabrication, photoluminescence and photocatalytic applications. J Alloy Compd 695:1029–1037